Basic study on active acoustic shielding: phase 6 improving the method to enlarge AAS window-2

Tatsuya MURAO[1]; Masaharu NISHIMURA[2]; Kazunori SAKURAMA[3]; Shin-ichiro NISHIDA[4]

[1,2,3,4] Tottori University, Japan

ABSTRACT

In this paper, it was proved to be useful to use M[(1-1)-L'] FX-LMS algorism for Active Acoustic Shielding (AAS) window to enlarge the window size. The AAS is a system that can attenuate the sound passing though an open window. The AAS system is composed of many AAS cells set in an array. Each AAS cell consists of approximately colocated a microphone and a speaker. However, a size of existing type AAS window is 250mm square. Therefore, we proposed M[(1-1)-L'] FX-LMS algorism(M: number of AAS systems, L': number of error signals used for controlling one AAS cell) for controlling a large size window and large number of AAS cells. This algorithm is a kind of FX-LMS algorithm, each AAS cell is controlled individually by it's own reference microphone and neighboring error sensors. In the previous work, 6 AAS cells is set on rectangular window (125 x 750mm square) and controlled by 6[(1-1)-3'] FX-LMS. As a result, this system was proved to be useful for controlling AAS cells, In this paper a simulator of M[(1-1)-L'] FX-LMS algorithm was constructed, and the simulation results by 6[(1-1)-3'] FX-LMS algorithm well coincided with the above experimented results. This suggests that large AAS window feasible.

Keywords: Active noise control, , Active acoustic shielding I-INCE Classification of Subjects Number(s): 38.2

1. INTRODUCTION

Active noise control (ANC) has been developed and successfully applied to machines such as air conditioning ducts, engine mufflers, ear protectors, car cabins, noise barriers and so forth. However, to reduce random noise in large spaces, ANC requires a multichannel system that is too complicated and costly to be practically applied. The applications of ANC to three-dimensional spaces are restricted to reducing rather simple type of noise such as booming noise in cars and propeller noise in airplane cabins (1,2). Therefore, a system for decentralized control has been proposed and developed, in which the boundaries of a sound field are controlled by distributed ANC units to reduce noise in the field (3-6). In this system, the acoustic impedance of the walls, namely, the sound absorption, sound insulation or sound diffraction of the walls, is controlled by distributed active cells containing one microphone and one speaker each. The crosstalk components of each active cell are so small that the cells can be individually controlled. Thus, we can control a sound field by placing active cells with the same performance side by side. This system is very simple, and an active soft edge (ASE) system has already been practically used to reduce the sound diffraction of noise barriers (4).

On the other hand, there is high demand for the development of open windows that can insulate sound by using ANC techniques. Ise proposed a sound field control method that controls the sound pressure and particle velocity at the boundary of the field (7). However, this system requires multiple channel control, making it too complicated to be practically used. The authors have been developing a decentralized control system that can reduce sound from visible sound sources such as traffic noise by using directional microphones and directional speakers (8). However its noise-reducing performance was unsatisfactory. Roure et al. also developed a noise shielding system for aircraft noise using directional devices (9). In this case, the quiet zone was small and the system was ineffective for sounds

[1] d12t1001h@edu.tottori-u.ac.jp
[2] mnishimura@mech.tottori-u.ac.jp
[3] sakurama@mech.tottori-u.ac.jp
[4] nishida@mech.tottori-u.ac.jp

of oblique incidence. With this research background, we proposed the concept of active acoustic shielding (AAS) and demonstrated its feasibility by performing some simple simulations and experiments (10). Then, a small AAS window of size in 250mm square was manufactured and installed in the door of an anechoic room. The noise attenuation resulting from AAS was measured for the noise transmitted through the window from outside the room. The effect on the noise reducing performance was examined for oblique incident sound, multiple noise sources, moving noise sources and sound reflection in the room (10). Moreover, improve of noise reducing performance in the low frequency region was obtained by AAS Type-3 which consisted of two kinds of AAS units (11,12). However, previous AAS-units were set on a small window. It is necessary to use more AAS cells for a large window and to improve the control method. Therefore, we proposed a new control method M[(1-1)-L'] FX-LMS for increasing AAS cells. In this method, each AAS cell is controlled individually and each control filter for ANC is adaptively converged by its own reference signal and neighboring error signals. In the previous work, a rectangular AAS window (125 x 750mm square) with 6 AAS cells was fabricated, and the method was examined. As the result, 6[(1-1)-3'] FX-LMS algorithm was proved to be able to converge each control filter by an error-scanning method to minimize the mean square of neighboring error signals (13). In this paper a simulator of M[(1-1)-L'] FX-LMS algorithm was constructed, and the simulation results by 6[(1-1)-3'] FX-LMS algorithm well coincided with the above experimented results. This suggests that large AAS window feasible.

2. BASIC CONCEPT AAS

According to Huygens' principle, a sound wave propagates by generating element waves at the wavefront and the intensity and direction of the sound wave are determined by the manner by which element waves are generated. If we can generate antiphase element waves with the same amplitude as the primary element waves at an arbitrary boundary plane, anti-sound waves will propagate behind the plane. Therefore, it is supposed that point sound sources distributed sufficiently closer to each other than the wavelength of the target sound can generate a wavefront of any shape by controlling their amplitudes and phases appropriately. This means that if we can make an active control system constructed with many noise controlling cells which have a collocated reference microphone and a control speaker individually and are distributed on an acoustic boundary such as a window at a sufficiently short distance from each other, the system can attenuate primary sound by generating an anti-phase sound relative to that measured by the reference microphone. We call this system "active acoustic shielding (AAS)".

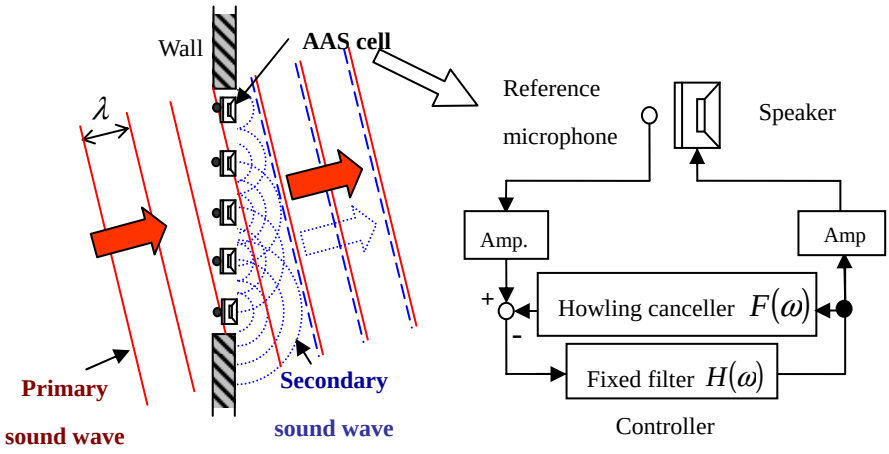

Figure 1 – Basic concept of Active Acoustic Shielding (AAS)

The basic concept of AAS is shown in Figure. 1. AAS cells are set in lines at an open window. An AAS cell has a reference microphone as close as possible in front of a secondary sound source. The signal measured by the reference microphone is inputted to the secondary source through a fixed filter $H(\omega)$. Namely, AAS cells are controlled by a feedforward method. The filter $H(\omega)$ is the same in every AAS cell. The transfer function of the filter $H(\omega)$ is determined so that most of the sound transmitted through the window is reduced. If necessary, a howling compensation filter $F(\omega)$ is set

in the AAS cells. Because the reference microphone and secondary source are nearly collocated, not only normally incident plane waves but also obliquely incident plane waves, spherical waves and waves with arbitrary shapes are expected to be reduced by AAS using the same filter $H(\omega)$, according to Huygens' principle. That means that AAS is expected to be effective for multiple primary sound sources and moving sources.

3. CONTROL OF BASIC AAS

Each AAS cell is finally controlled individually by multiplying each measured reference signal by a fixed transfer function $H(\omega)$ and inputting it to each secondary speaker as shown in Figure 1. In the experiment $H(\omega)$ was determined as follows. At first, each error microphone is placed behind each AAS cell at the distance d ($\approx w$: span of AAS cells). The system is controlled by the 4(1-1)-4 Filtered-X-LMS algorithm shown in Figure 2.

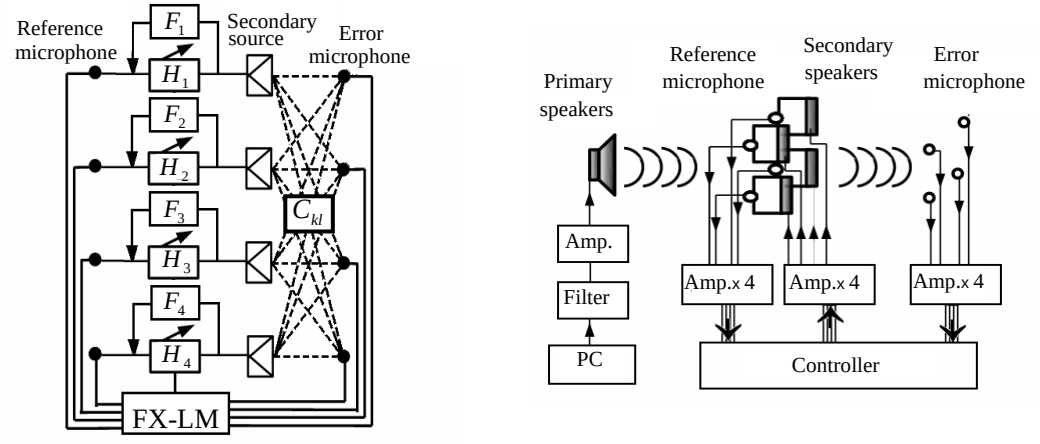

Figure 2 – 4(1-1)-4 Filtered-X-LMS algorithm

This is equivalent to the algorithm with no cross-filters in the ordinary 4-4-4 Multiple Filtered-X-LMS algorithm (10). The characteristic of this system is that each secondary source can only be actuated by its own reference signal. $H_1(\omega)$ to $H_4(\omega)$ are adaptively converged by the error-scanning method so that the mean square of every error signal is minimized. Next, after confirming that each transfer function is similar, we select one representative transfer function and input it to each AAS cell. Thus each AAS cell has the same transfer function. In this case, the nearly same noise reduction could be obtained as in the case of adaptive filters.

This control method can be theoretically applied for the case of more AAS cells. However, it is unrealistic because controllers become expensive to calculate a lot of error signals.

4. NEW ALGORITHM FOR INFINITE AAS CELLS

It is considered that the only signals of error microphones neighboring to every secondary source are important for constructing its controlling filter, and the information of error microphones set far away from the secondary source are not important. Then we propose the following M[(1-1)-L'] FX-LMS algorithm.

Figure3 shows M[(1-1)-L'] FX-LMS algorithm. M is number of AAS system, L' is number of error signals used for controlling one AAS cell (L' = 3 in Figure 3).

Process or this algorithm is as follows. First, each AAS cell, every transfer function of the error path $C_{kl}(\omega)$ from k control speaker to l error microphone is identified by using white noise. Secondly, the transfer functions from $H_1(\omega)$ to $H_M(\omega)$ are adaptively converged by the error-scanning method to minimize the mean square of every error signal, by using the neighboring error signals and the filtered reference signal (for example in Figure 3, L'=3, number m of AAS cell uses signals of $e_{m-1}(n)$, $e_m(n)$, $e_{m+1}(n)$, $c_{m,m-1} * x_m(n)$, $c_{m,m} * x_m(n)$ and $c_{m,m+1} * x_m(n)$). The equation of adaptive FIR filter $\mathbf{h}_m(n)$ is written as follows,

$$\mathbf{h}_{jk}(n+1) = \mathbf{h}_{jk}(n) + \mu \cdot \sum_{l=m-P}^{m+P} \mathbf{r}_{jkl}(n) \cdot e_l(n) \qquad \left(j = k = m \quad , P = \frac{L'-1}{2}, 0, < l < M \right) \tag{1}$$

$$\mathbf{h}_{jk}(n) = \left[h_{jk}^{(0)}(n) \quad h_{jk}^{(1)}(n) \quad \cdots \quad h_{jk}^{(hl)}(n) \right]^T \qquad (hl : Number \quad of \quad TAP) \tag{2}$$

$$\mathbf{r}_{jkl}(n) = \left[r_{jkl}(n) \quad r_{jkl}(n-1) \quad \cdots \quad r_{jkl}(n-hl+1) \right]^T \tag{3}$$

$$r_{jkl}(n) = x_j(n) * \hat{c}_{kl} = \sum_{a=0}^{\hat{c}l-1} x_j(n-a) \cdot \hat{c}_{kl}^{(a)} \cong \mathbf{x}(n)^T \hat{\mathbf{c}}_{kl} \qquad (\hat{c}l : Number \quad of \quad TAP) \tag{4}$$

$$\mathbf{x}_j(n) = \left[x_j(n) \quad x_j(n-1) \quad \cdots \quad x_j(n-\hat{c}l) \right]^T \tag{5}$$

$$\hat{\mathbf{c}}_{kl} = \left[\hat{c}_{kl}^{(0)} \quad \hat{c}_{kl}^{(1)} \quad \cdots \quad \hat{c}_{kl}^{(\hat{c}l-1)} \right]^T \tag{6}$$

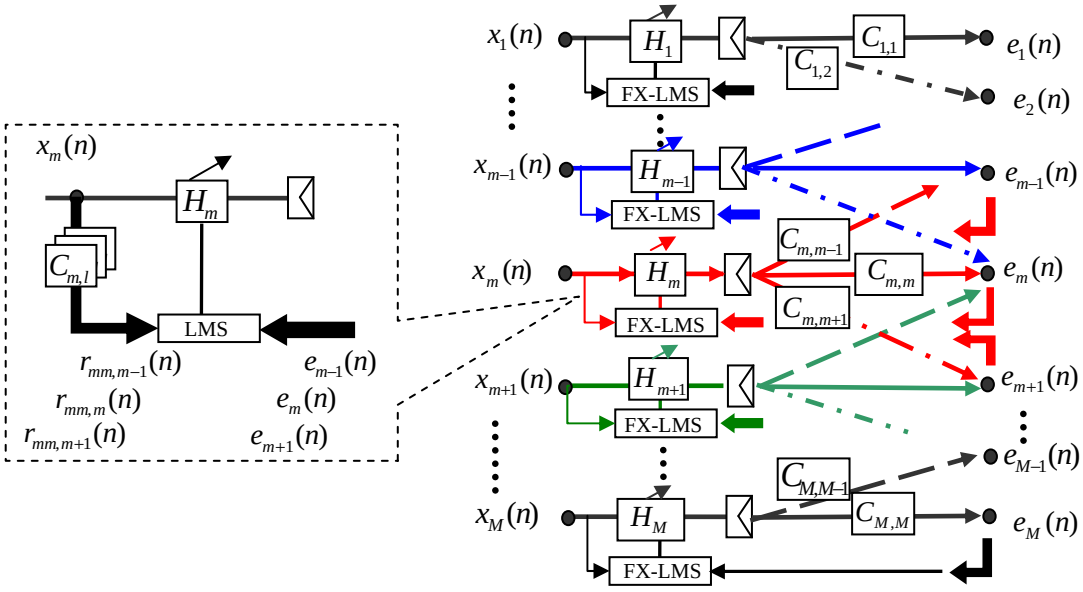

Figure 3 – M[(1-1)-L'] Filtered-X-LMS algorithm

Each AAS cell adapt individually and simultaneously. After convergence, each adaptive FIR filter $\mathbf{h}_m(n)$ is fixed and all error microphones remove. Finally, each AAS cell with one reference microphone and one speaker individually is controlled by each fixed FIR filter.

5. SIMPLE EXPERIMENT

A simple two dimensional model was fabricated and examined experimentally by M[(1-1)-L'] FX-LMS algorism for simplicity. This model has 6 AAS cells in line on a narrow rectangular window (L'=3, M=6).

5.1 Fabrication of AAS Window for New Algorithm

A rectangular window with a 125mm x 750mm opening containing six AAS cells was manufactured as shown in Figure 4.

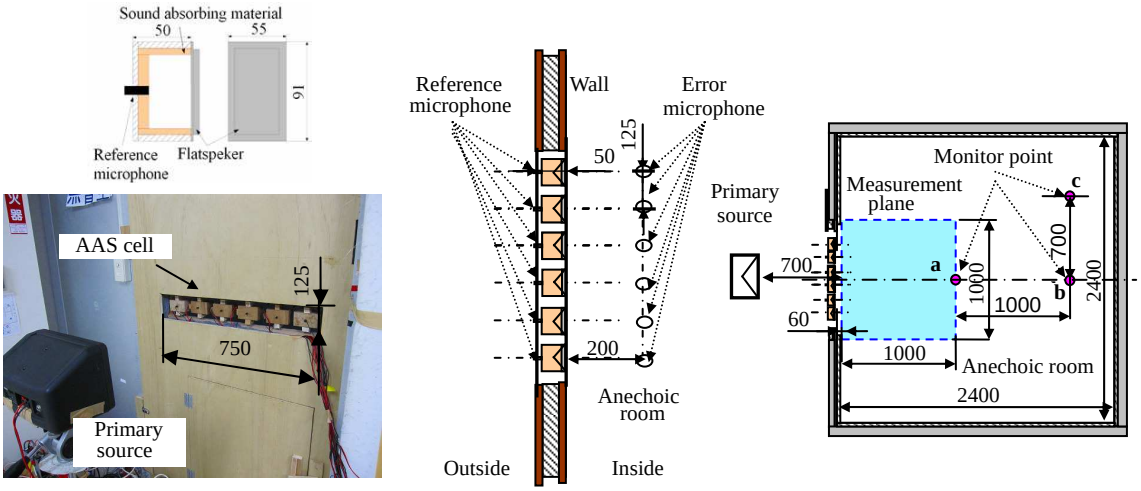

(a) AAS cell and outside view (b) Plane view (c) measurement zone

Figure 4 – Fabricated model of rectangular AAS window

In this study, the target frequency range of the sound to be attenuated is regarded from 500Hz to 2kHz. A flat speaker was used as a secondary source because of its quick response. The reference microphone was set immediately behind the speaker box. The distance between the reference microphone and the speaker diaphragm is only 50mm. The distance is considered to be enough short for the sound whose frequency is below 2kHz, because it is shorter than a quarter of the wavelength. This AAS cell is controlled by a feed-forward method as described below. In this case, the causality of the signals was proved to be satisfied in our previous report despite the short distance (10).

The distance between each cell center w is 125mm. This means that w/λ = 0.184－0.735 for the target frequency range. According to our previous report, the condition w/λ =0.75 enables a quiet zone to develop behind the AAS plane in the case of sound with normal incidence. The open area ratio of the AAS window is 68%.

5.2 Control of AAS Window

Each AAS cell is controlled individually by multiplying each measured reference signal by a fixed transfer function $H_m(\omega)$ and inputting it to each secondary speaker as shown in Figure 1. In the experiment $H_m(\omega)$ was determined as follows.

Firstly, each error microphone was placed 200mm behind each AAS cell as shown in Figure 4(b), and the system was controlled by the 6[(1-1)-3’] filtered-X-LMS algorithm. EX-tool (Redec) was used as the controller. In this case, an AAS cell generally uses only its own reference microphone signal and three neighboring error microphone signals.

5.3 Test Setup

Figure 4 shows the rectangular AAS window installed at the door of a small anechoic room. A primary source generating frequency restricted random noise from 500Hz to 2000Hz was set 700mm in front of the AAS-cells. The adaptive control in each cell was conducted simultaneously and individually. After each filter $H_m(\omega)$ was converged, each filter was fixed and each cell controls individually at the same time. In this experiment, the sampling frequency f_s of the controller is 48kHz, and the filter tap lengths of $H_m(\omega)$ and the error path filter $C_{kl}(\omega)$ are 200. The sound pressure spectra at error microphones and fixed points a, b and c shown in Figure 4 (c) were measured with and without ANC (ANC ON and OFF). Moreover, 1/3-octave-band sound pressure level contours and sound attenuation level contours were drawn on the horizontal plane (1m x 1m) at the center height of the AAS-Window, as shown in Figure 4 (c).

5.4 Test Results

Figure 5 shows the relative sound pressure spectra at the error microphone point **3** and fixed point **a** under the conditions of ANC ON and OFF. Figure 6 shows 1/3-octave-band sound pressure level contours and sound attenuation level contours at 1000Hz. In Figure 6, blue dots show points of each error microphone. This figure shows that a large amount of noise reduction (10 -15dB) was obtained in the target frequency range (500Hz-2kHz) on each error microphone, each fixed point and over a wide area of the test room.

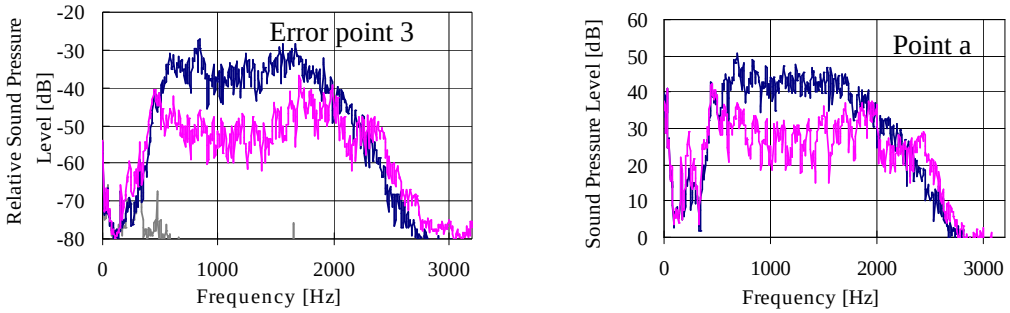

Figure 5 – The relative sound pressure spectrum at the error point and sound pressure spectrum at the fixed point under the condition of ANC ON and OFF

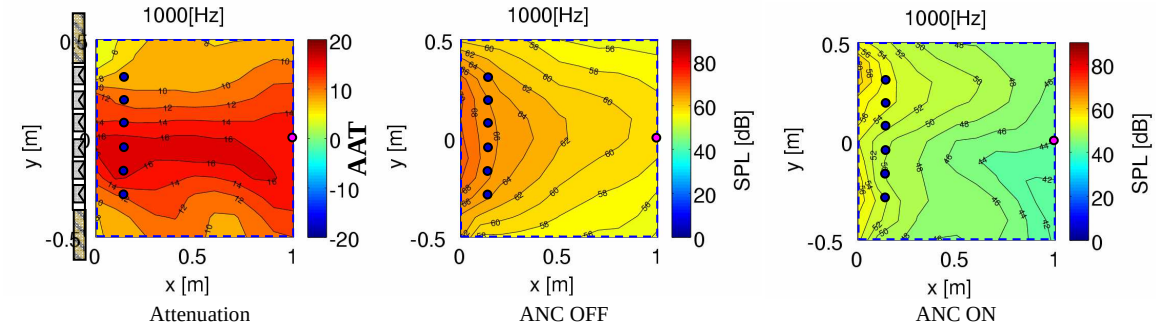

Figure 6 – Typical 1/3-octave-band sound attenuation level contours and sound pressure level contours under the condition of ANC ON and OFF

6. SIMULATION OF NEW ARGOLITHM FOR AAS

In this paper, we simulate the M[(1-1)-L'] Filtered-X LMS algorithm using simulation software (MATLAB) by numerical calculation . Figure 7 shows the model of simulation. We made a software program satisfying equations in chapter 4.

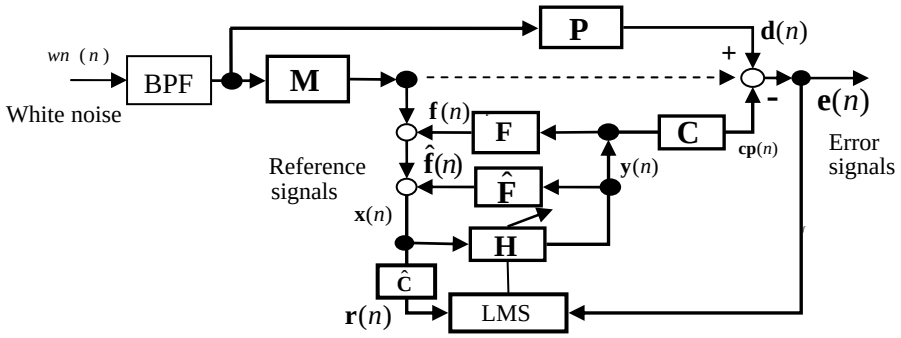

Figure 7 – Simulation model

The simulation used transfer functions measured in the simple experiment shown in chapter 5. Each transfer function was measured under actual acoustic field. In Figure 7, **P** is primary paths, **M** is paths between a primary source to reference signals, **C** is error paths, **F** is feedback paths, $\hat{\mathbf{C}}$ and $\hat{\mathbf{F}}$ is identified paths, **H** is control filters. At first, we constructed the program based on the full channel multiple filtered-X LMS algorithm. Each capital symbol has matrix and include all coefficients of each filter [e.g. **H** include $\mathbf{h}_{jk}(n)\left(j=1,2,\cdots J, k=1,2,\cdots K\right)$]. After that, coefficients of particular filters $\mathbf{h}_{jk}(n)\left(j\neq k\right)$ and $\mathbf{c}_{kl}\left(k\neq l\pm p,\, p=0,1,\cdots(L-1)/2\right)$ were set 0 to eliminate the filters. White noise with band path filter (500 Hz~2 kHz) was used as the primary source.

6.1 Conditions

Simulations parameters show as follow. Sampling frequency is 48 kHz, cutoff frequency of the antialiasing filter is 20 kHz and step size parameter is 0.000003. Table 1 shows sizes of previously-identified filters.

Table 1 – Size of identified filters

J=K=L=6	**P**	**M**	**F**	**C**
Number of tap	600	600	600	500
Size of matrix	L×P_tap	J×M_tap	K×J×F_tap	K×L×C_tap

In this paper, Howling cancel filter **F** was not used as the same condition of the examinations. Table 2 shows simulation conditions and size of filters.

Table 2 – Conditions and size of filters

Condition Number	**H**	$\hat{\mathbf{C}}$	algorithm
Experiment case 0	200	200	6[(1-1)-3'] ch
Simulation case 1	200	200	6[(1-1)-3'] ch
Simulation case 2	600		
Simulation case 3	1200		
Simulation case 4	200	500	6[(1-1)-3'] ch
Simulation case 5	600		
Simulation case 6	1200		
Simulation case 7	200	200	6[(1-1)-6'] ch
Simulation case 8	600		
Simulation case 9	600	500	
Simulation case10	200	200	6 Full ch
Simulation case 11	600		
Simulation case 12	600	500	

6.2 Simulation Result

Figure 8 to 11 shows the relative sound pressure spectra at the error microphone point 3 and 6 under the conditions of ANC ON and OFF. Table 3 shows conditions of simulation on Figure 8 to 11.

Table 3 – Simulation conditions

Condition	**Figure 8**	**Figure 9**	**Figure 10**	**Figure 11**
Cases	0,1,2,3,4	0,2,5	0,1,7,10	0,5,9,12
Fixed parameter	Algorithm, **C**	Algorithm, **H**	**H: 200, C:200**	**H: 600, C:500**
Variable	**H**	**C**	**Algorithm**	**Algorithm**

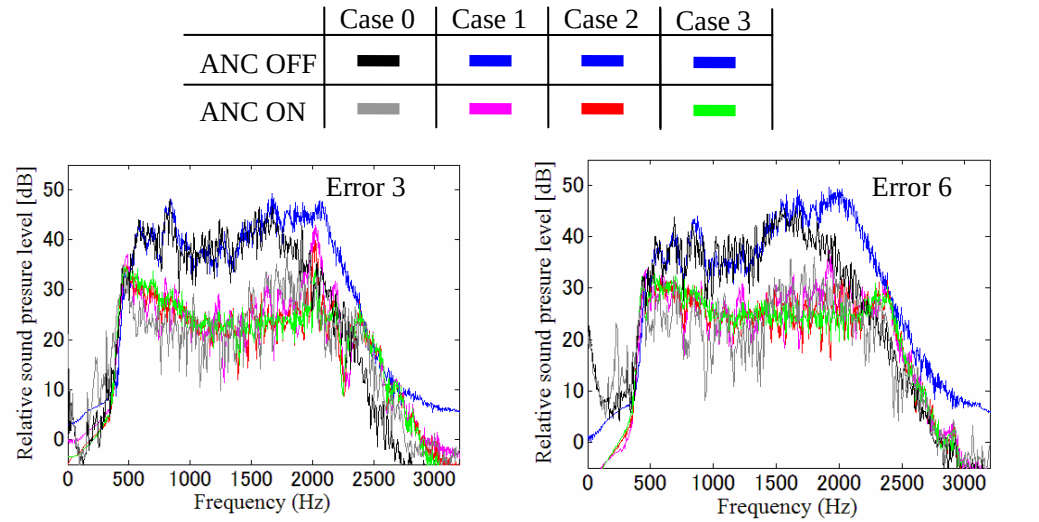

Figure 8 – The relative sound pressure spectrum at the error point and sound pressure spectrum at the fixed point under the condition of ANC ON and OFF in Case 0, 1, 2 and 3

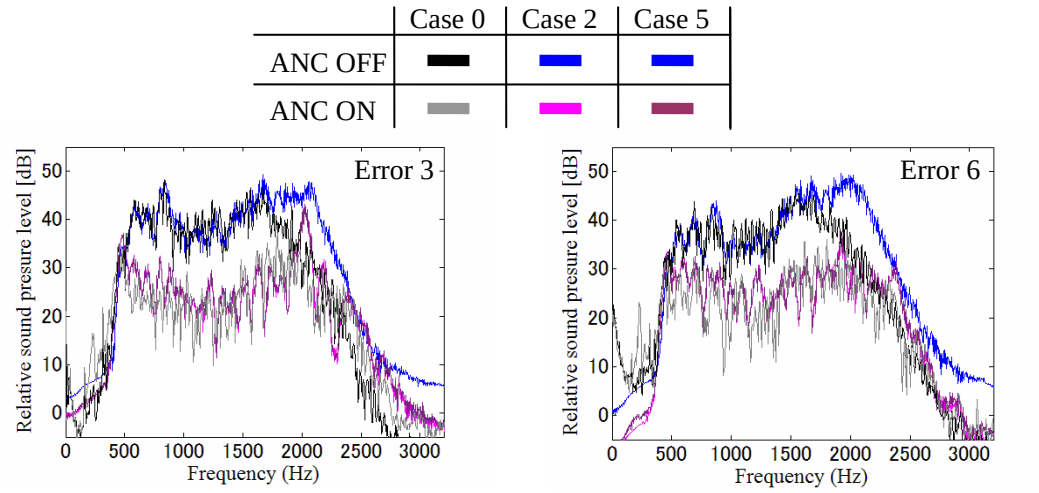

Figure 9 – The relative sound pressure spectrum at the error point and sound pressure spectrum at the fixed point under the condition of ANC ON and OFF in Case 0, 2 and 5

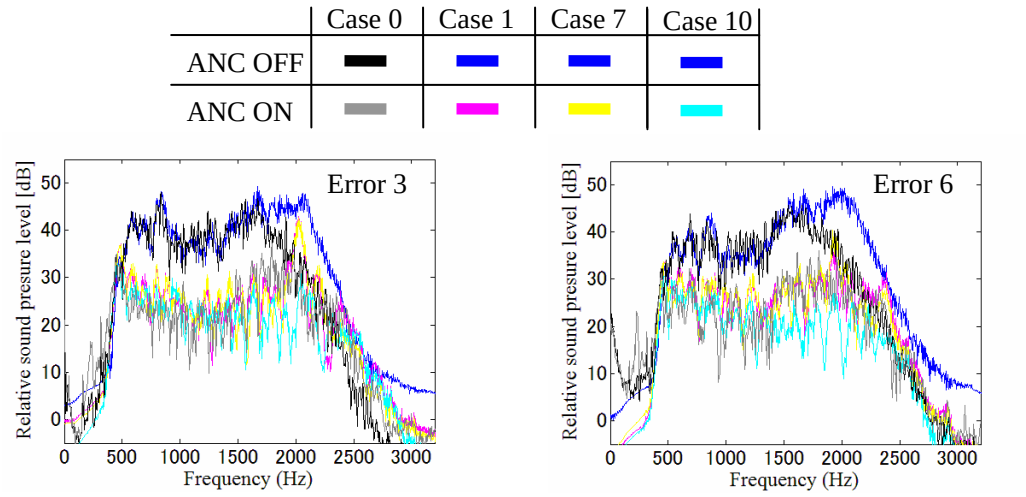

Figure 10 – The relative sound pressure spectrum at the error point and sound pressure spectrum at the fixed point under the condition of ANC ON and OFF in Case 0, 1, 7 and 10

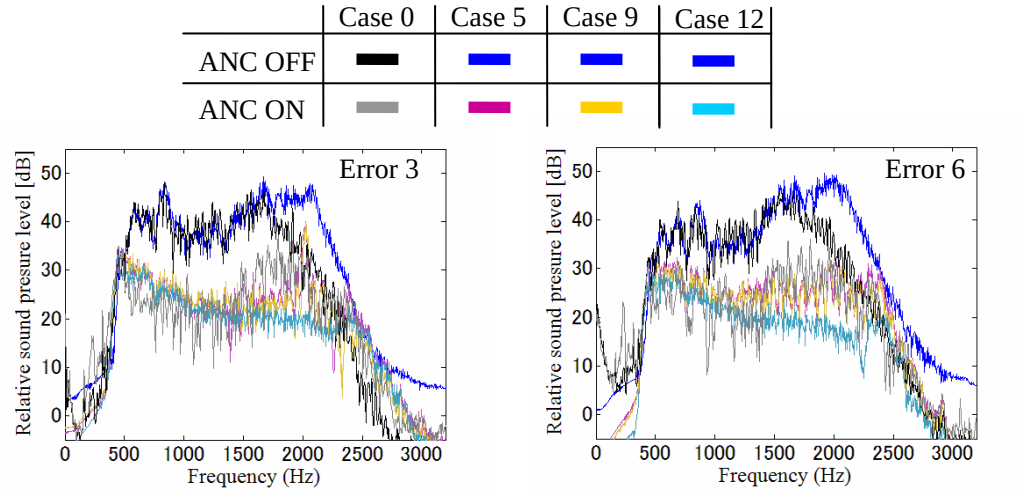

Figure 11 – The relative sound pressure spectrum at the error point and sound pressure spectrum at the fixed point under the condition of ANC ON and OFF in Case 0, 5, 9 and 12

6.3 Discussion

6.3.1 Condition 1

Figure 8 shows relative sound pressure spectra under condition 1. It was used 6[(1-1)-3'] FX LMS algorithm, the size of filter $\hat{\mathbf{C}}$ was fixed to 200 taps and as the same size as that of the experiment in chapter 4. The conditions of case 1 are the same as those of case 0 (experiment), and both results are similar. This proves the validity of the simulation. In this figure, the size of **H** was changed from 200 to 600 and 1200 taps, to examine the influence of the size of **H** on sound attenuation. This figure shows that the influence of the size of **H** is not so much.

6.3.2 Condition 2

Figure 9 shows the influence of the size of filter $\hat{\mathbf{C}}$ on sound attenuation. It is also not large.

6.3.3 Condition 3 and 4

Figure 10 and 11 shows relative sound pressure spectra under condition 3 and 4. These figures compare the effect of different algorithms 6[(1-1)-3'], 6[(1-1)-6'] and 6 channel full FX LMS. 6[(1-1)-3'] and 6[(1-1)-6'] show the similar noise reduction about 10~15dB in the target frequency range 500 Hz ~ 2 kHz. It shows that 3 neighboring error microphones are enough in this configuration. However, the 6ch Full MFX-LMS shows larger noise reduction from 1.5 kHz to 2 kHz. This shows importance of the cross filters of **H.**

7. CONCLUSIONS

A new M[(1-1)L'] FX-LMS algorithm was proposed for controlling AAS (Active Acoustic Shielding), which use only neighboring error microphones. And its usefulness was examined by simple was examined by simple experiment and simulations. The following conclusions were obtained.

1. A simulator of this algorithm was constructed and proved its validity by comparing with the experimental results.

2. This algorithm was proved to be able to converged the adaptive control filter by experiment and simulations

3. AAS-window can be enlarged infinitely by using this algorithm.

REFERENCES

1. Kuo M S, and Morgan R D, Active Noise Control Systems, Wiley, (1996)
2. Sano H, and Adachi S, “Two-Degree-of-Freedom Active Control of Road Noise inside Automobiles”, Proc. of ACTIVE97, pp. 543-546, (1997)
3. Nishimura M, Ohnishi K, Patrick P W and Zander C A, “Development of Active Acoustic Treatment (Phase 1; Basic Concept and Development of AAT-Cell”, Proc. of ACTIVE 97, pp. 319-330, (1997)
4. K. Ohnishi, T. Saito, S. Teranishi, Y. Namikawa, T. Mori, K. Kimura, and K. Uesaka, “Development of the Product-type Active Soft Edge Barrier”, Proc. of ICA 2004, Ⅱ1041-1044, (2004)
5. M. Nishimura, T. Goto, and N. Kanamori, “Basic Research on Active Sound Insulation Unit”, Proc. of ICA 2004, pp. Ⅲ2169-2172, (2004)
6. P. Gardonio, “Sensor-Actuator Transducers for Smart Panels”, Proc. of ACTIVE 2006, CD-ROM, (2006)
7. S. Ise, “A Principle of Sound Field Control Based on the Kirchhoff-Helmholtz Integral Equation and Theory of Inverse System”, Proc. of Acoustica 85, pp.78-87, (1999)
8. M. Nishimura, K. Ohnishi, N. Kanamori, and Y. Umebayashi, “Feasibility Study on Active noise Control for Moving Sources in the Open Field , Using Directional Microphones and Directional Speakers”, Proc. of ACTIVE 2006, CD-ROM, (2006)
9. A. Roure, P. Herzog, and C. Pinhede, “Active Barrier for Airport Noise”, Proc. of INTER-NOISE 2006, CD-ROM, (2006)
10. Murao.T., Nishimura, M., Basic Study on Active Acoustic Shielding, Proceeding of Journal of Environment and Engineering, Vol.7, No.1 (2012a).
11. T.Murao and M.Nishimura, “Basic Study on Active Acoustic Shielding: Phase 3 Improving Noise Reducing Performance in Low Frequency Region”, Proc. of INTER-NOISE 2011, CD-ROM, (2011)
12. T.Murao, M.Nishimura and K.Sakurama, “Basic Study on Active Acoustic Shielding: Phase 4 improving noise reducing performance in low frequency-2”, Proc. of INTER-NOISE 2012, CD-ROM, (2012)
13. .T.Murao, M.Nishimura and K.Sakurama, “Basic Study on Active Acoustic Shielding: Phase 5 iimproving decentralized control algorithm to enlarge AAS window”, Proc. of INTER-NOISE 2013, CD-ROM, (2013)